OFFICIAL ORGAN OF THE RADIATION RESEARCH SOCIETY

RADIATION RESEARCH

EDITOR-IN-CHIEF: DANIEL BILLEN

Volume 83, 1980

ACADEMIC PRESS

New York London Toronto Sydney San Francisco

MADE IN THE UNITED STATES OF AMERICA

RADIATION RESEARCH

OFFICIAL ORGAN OF THE RADIATION RESEARCH SOCIETY

VOLUME 83, 1980

Councilors Radiation Research Society 1980–1981

PHYSICS

M. Inokuti, Argonne National Laboratory

H. J. Burki, University of California, Berkeley

BIOLOGY

J. S. Rasey, University of Washington

A. M. Rauth, Ontario Cancer Institute, Toronto, Canada

MEDICINE

H. D. Suit, Massachusetts General Hospital

J. A. Belli, Harvard Medical School

CHEMISTRY

J. F. Ward, University of California, San Diego

M. Z. Hoffman, Boston University

AT-LARGE

L. A. Dethlefsen, University of Utah

R. M. Sutherland, University of Rochester

CONTENTS OF VOLUME 83

NUMBER 1, JULY 1980

NUMBER 2, AUGUST 1980

NUMBER 3, SEPTEMBER 1980

The Subject Index for Volume 83 will appear in the December 1980 issue as part of a cumulative index for the year 1980.

RADIATION RESEARCH 83, 511–528 (1980)

Biophysical Studies with Spatially Correlated Ions

4. Analysis of Cell Survival Data for Diatomic Deuterium[1]

ALBRECHT M. KELLERER, YUK-MING P. LAM,* AND HARALD H. ROSSI*

*Institut für Medizinische Strahlenkunde der Universität Würzburg, Würzburg, West Germany, *Radiological Research Laboratory, Department of Radiology, Cancer Center/Institute of Cancer Research, Columbia University College of Physicians and Surgeons, New York, New York 10032*

KELLERER, A. M., LAM, Y. M. P., AND ROSSI, H. H. Biophysical Studies with Spatially Correlated Ions. 4. Analysis of Cell Survival Data for Diatomic Deuterium. *Radiat. Res.* **83**, 511–528 (1980).

An analysis is given of previously reported results of experiments in which cells have been irradiated with pairs of ions of variable mean separation. These studies were motivated by the theory of dual radiation action and specifically by the postulate that the lesions responsible for cell impairment by ionizing radiation are formed by the combination of pairs of sublesions that are molecular alterations produced by individual energy transfers in the cell nucleus. It is concluded that the observations are consistent with dual radiation action, and the most striking finding is that there appears to be a bimodal distribution of interaction distances with maxima at less than 0.1 μm and more than 1 μm. Single tracks cause primarily the lesions produced in short-range interactions but they also contribute, at least in late S phase, a relatively small proportion of the long-range interactions which are principally due to a two-track mechanism. The experiments suggest that the radiation-sensitive components of the cell are arranged in a highly nonuniform pattern which may take the form of floccules having diameters of less than 100 nm.

INTRODUCTION

This is Part 4 of a series of four papers which constitute an interim report on a number of experiments, still in progress, on the biological effect of spatially correlated deuteron ions with a linear energy transfer (LET) of about 33 keV/μm. The earlier papers (*1–3*) will be referred to as papers 1 through 3. The reader is advised to consult paper 1 for the motivation of experiment, paper 2 for the physical setup, and paper 3 for the experimental procedure in the assessment of the survival of V-79 Chinese hamster cells and for the results. The present paper deals with the scheme for analyzing these cell survival data and demonstrates it by application to the limited amount of data collected so far. The reader is urged to bear in mind that the data and their analysis and interpretation are preliminary, as more and better data are being accumulated.

[1] The U. S. Government's right to retain a nonexclusive royalty-free license in and to the copyright covering this paper, for governmental purposes, is acknowledged.

0033-7587/80/090511-18$02.00/0

DUAL RADIATION ACTION

From the theory of dual radiation action it has been concluded that observed cellular effects are due to cellular lesions that are the result of the combination of pairs of sublesions (*4*). The purpose of the present experiments is a critical examination of this conclusion and, in particular, a determination of the conditions for the combination of sublesions. In the earlier treatment it has, for simplicity, been assumed that sublesions are formed within certain spherical sites in the cell and that the combination probability of two sublesions is independent of their distance, provided both sublesions occur within the site. With this assumption it was concluded from a comparison of various effects produced by neutrons with those produced by sparsely ionizing radiations that combination of sublesions can take place over distances of the order of one or several micrometers. However, it is apparent that the combination probability of sublesions cannot, in reality, be independent of their separation. The site model is therefore an oversimplification, and a generalized formulation of dual radiation action has recently been given that takes into account a more complex geometry of the sensitive structures in the cell and a distance dependence of the combination probability of sublesions that are formed in these sensitive structures (*5*). This generalized formulation will in the following be applied to obtain conclusions concerning these two geometrical factors.

Energy transfers from ionizing radiations to the irradiated medium occur at discrete points which are termed *transfer points*.[2] Two conditions have to be met if a pair of energy transfers is to produce sublesions which will then combine to create a lesion. First, the transfers have to occur in the sensitive structures in the cell where sublesions can be produced; these sensitive structures are postulated to extend over the entire nucleus, although only a portion of the nuclear volume, termed the *matrix*, can yield sublesions. Second, the energy transfers have to be close enough in distance that a pair of sublesions that may be produced can combine to form a lesion. Accordingly the probability $p(x)$ that two energy transfers ϵ_1 and ϵ_2 form sublesions that will produce a lesion depends on two functions $s(x)$ and $g(x)$:

$$p(x) = k \cdot \epsilon_1 \cdot \epsilon_2 \cdot \frac{s(x) \cdot g(x)}{4\pi\rho x^2} . \qquad (1)$$

The function $s(x)$ is termed the geometric proximity function and depends only on the configuration of the matrix. $s(x)dx$ is the expected mass of the matrix in a spherical shell of radius x and thickness dx that is centered at a point randomly chosen in the matrix.[3] The second function $g(x)$ is the probability that sub-

[2] An energy transfer is energy locally imparted to the medium; it is equal to the kinetic energy of the ionizing particle that undergoes an interaction at the transfer point minus the kinetic energy of any ionizing particle(s) emerging from the reaction. Changes of rest mass are here disregarded, if they occur the definition is somewhat more complicated (*6*, *7*).

[3] $s(x)/4\pi\rho x^2$ is equal to the quantity that has been called geometric reduction factor of a volume by Berger (*18*). It is equal to the probability that a point is in the matrix if it is separated by the distance x from a random point in the matrix. In the earlier treatment (*5*) $s(x)$ had been given the dimension volume (instead of mass) divided by length. However, inclusion of the density ρ of the matrix simplifies some of the formulae.

lesions separated by the distance x do in fact combine. Equation (1) has been obtained earlier (*5*); it is here presented without derivation.

Experimental results will not usually provide information on the two functions $s(x)$ and $g(x)$ separately. Inferences can, however, be drawn that relate to their product, and it is therefore practical to introduce the function

$$\gamma(x) = \frac{s(x)g(x)}{4\pi\rho x^2} \Big/ \int_0^\infty s(x)g(x)dx. \tag{2}$$

$\gamma(x)$ determines, according to Eq. (1), the probability of two energy transfers separated by the distance x to produce a lesion. The normalization of the function is arbitrary as Eq. (1) contains a constant that cannot, in general, be determined experimentally. Nevertheless, the convention in Eq. (2) that gives $\gamma(x)$ the dimension of a reciprocal mass is practical [see Eq. (4)]. The evaluation of the function $\gamma(x)$ is the ultimate aim of this series of experiments.

If a medium is exposed to ionizing radiation one deals with a distribution of distances between transfer points. This (nonnormalized) distribution $t(x)$, termed the energy proximity function, is defined in a manner analogous to that of $s(x)$. However, the function relates not to the geometry of the matrix, but to the geometry of the charged particle tracks. $t(x)dx$ is the expected energy imparted to a spherical shell of radius x and thickness dx that is centered at a transfer point which is randomly chosen. Only energy imparted due to the same particle and/or its secondaries and associated particles is considered in the definition of $t(x)$.

With these definitions one obtains, as shown earlier (*5*), a formula for the total yield of lesions at the absorbed dose D:

$$\epsilon(D) = k(\xi D + D^2), \tag{3}$$

with

$$\xi = \int_0^\infty \gamma(x)t(x)dx. \tag{4}$$

k is a factor that can be related to various quantities. One of these is LET. However, it may be assumed that in these experiments k is independent of track separation. This is supported by data of Bird and Kliauga,[4] who have found in track-segment experiments on V-79 cells that this coefficient shows no detectable variation between LET values 30 to 65 keV/μm.

The strategy of the molecular ion experiment is to change the function $t(x)$ by exposing the cells to pairs of deuterons with different mean separations. Analysis of cell survival resulting with different mean separations will then provide information on the function $\gamma(x)$. In the studies carried out thus far only three different values of the mean deuteron separation have been utilized (*3*). However, it will be seen that even these limited results permit significant conclusions.

Recent studies (*8*) have shown that correlated ions also have higher effectiveness in the production of chromosome aberrations. However, this analysis is restricted to cell survival studies only.

[4] R. P. Bird and P. J. Kliauga, Irradiations with the track segment facility and the analysis of data. Annual Progress Report, Radiological Research Laboratory, Columbia University, Report No. COO-4733-2, July 1979, p. 162.

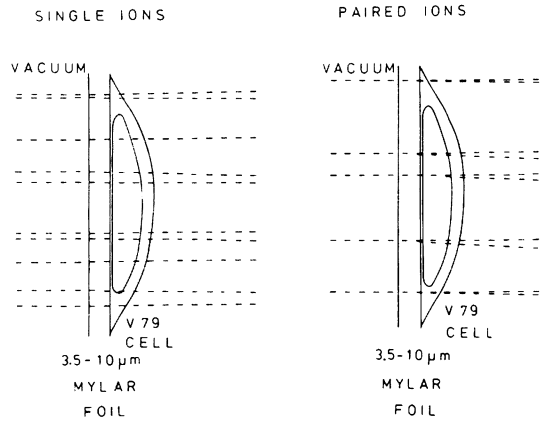

FIG. 1. Schematic diagram of V-79 Chinese hamster cells plated on thin Mylar foils and irradiated by single deuterons and pairs of correlated deuterons. Deuterons of LET approximately 33 keV/μm traverse the cells, either as single ions or as pairs of ions originating from a single molecule. The average lateral separation between the two correlated deuterons depends on the Mylar thickness.

GENERAL FEATURES OF THE ANALYSIS

In the experiments considered here, an event constitutes the passage of a single deuteron, a single ^{3}He ion, or a spatially correlated pair of deuterons through a cell. The last case results if, after breaking up in the supporting Mylar foil, the deuterons from a molecule pursue different paths through a cell nucleus, as illustrated in Fig. 1. If the distance between the two tracks at a depth midway through the cell nucleus is denoted by x, then the distribution in x is given by (*2, 9*)

$$d(x) = \frac{2x}{b} e^{-x^2/b^2}, \tag{5}$$

where b, termed the mean separation at median cell depth, is the root mean square of x, and is dependent on, among other things, the thickness of the Mylar foil. The ion tracks in the cell nucleus can be treated as parallel straight lines, and the LET along them is considered constant (*2*). The assumptions are met with adequate accuracy. A further simplification arises from the fact that, at the energies selected, the lateral extension of the track can be disregarded in comparison even to the smallest mean separations of the paired ions (*10*). These considerations make it unnecessary to utilize the results of detailed calculations of $t(x)$. For two parallel straight thin lines with constant LET (denoted by dashed lines in Fig. 1) the function $t_b(x)$ takes the form

$$t_b(x) = 2L\left[1 + \frac{2}{b^2}\int_0^x \frac{xs}{(x^2 - s^2)^{1/2}} e^{-s^2/b^2} ds\right]. \tag{6}$$

L is the linear energy transfer. Its value is 33 keV/μm for the deuterons applied in the present experiment.

The function $t_b(x)/L$ is plotted in Fig. 2 versus x/b. The values resulting from Eq. (4) for different values of b will be denoted by ξ_b. From Eq. (6) it follows that $t_b(x)$ and consequently ξ_b differs by a factor of 2, for $b = \infty$ and $b = 0$.

While $t(x)$ is determined by the physical aspects of the irradiation, the values ξ in Eq. (3) are derived from the biological results. Cell survival curves are fitted to the expression

$$S = e^{-\epsilon(D)} = e^{-k(\xi D + D^2)}. \tag{7}$$

The objective of the analysis is then to determine the function $\gamma(x)$ that is consistent with the observed values and the functions $t_b(x)$ associated with the values of b employed in the experiment

$$\int_0^\infty \gamma(x) t_b(x) dx = \xi_b. \tag{8}$$

This includes also the value $b = \infty$, i.e., the case of random incidence of deuterons (breakup foil in place). Furthermore, an experiment with uncorrelated ^{3}He ions of linear energy transfer 65 keV/μm is included. This experiment serves as a substitute for the condition $b = 0$ which cannot be realized experimentally.

ANALYSIS OF THE EXPERIMENTAL DATA

To determine the value ξ_b corresponding to a certain Mylar thickness it is necessary to assess the cell survival for a number of doses and then to fit the resulting surviving fractions to Eq. (7). Because of unavoidable fluctuations of cellular sensitivity between experiments the dose–effect curves for different values of b should ideally be performed simultaneously with the same suspension of cells (*11*). This would guarantee that the resulting parameters are comparable. However, because of the experimental limitations, it was impossible to irradiate with more than one dose and one Mylar thickness on the same day.

For this reason a method has been chosen which permits the determination of the difference between ξ_b and ξ_∞ without the requirement to obtain full survival curves in one simultaneous experiment. The method consists in the determination of the values ξ_b from observed survival ratios. According to Eq. (7) one has

$$\ln (S_\infty / S_b) = \xi_b k D - \xi_\infty k D. \tag{9}$$

The values k and ξ_∞ are obtained from the full survival curves for the unpaired deuterons and He ions and ξ_b is then derived in a least-square fit including all observations for the mean separation b.

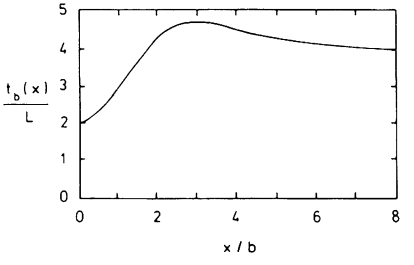

FIG. 2. The energy proximity function of a pair of correlated ions according to Eq. (6). The distance is normalized to the mean lateral separation b of the ions.

TABLE I

Parameters Resulting from the Fit of the Expression $\ln S = -\xi kD - kD^2$ to the Survival Data[a]

Mylar thickness (μm)	$b/\mu m$	*Late S phase* (α/Gy^{-1})	G_1/S *phase* (α/Gy^{-1})
$-(He^+)$	0	0.564 ± 0.027	0.762 ± 0.05
3.5	0.091	0.371 ± 0.042	0.448 ± 0.096
6.4	0.156	0.371 ± 0.041	0.434 ± 0.163
10	0.255	0.335 ± 0.044	0.436
$-(d^+)$	∞	0.278 ± 0.034	0.412 ± 0.066
		$k = (0.03 \pm 0.0041)\ Gy^{-2}$	$k = (0.069 \pm 0.012)\ Gy^{-2}$

[a] The corresponding values ξ are plotted in Figs. 5, 8, and 9. The least-squares fit has been performed with one value k for the cells in late S phase and one value for G_1/S cells. The resulting curves are given in Figs. 2 and 4.

The results of the analysis are summarized in Table I. The statistical method is performed with the usual least-squares method (*12*) in terms of the parameters k and $\alpha = k\xi$. Two cell ages, namely late S and G_1/S, and three foils of different thickness were studied, giving rise to six different combinations. The three thicknesses were 3.5, 6.4, and 10 μm and yielded values of 0.091, 0.156, and 0.255 μm, respectively, for the mean separation b of correlated deuteron ions at median cell depth [taken to be 3 μm deep (*2*)].

For each cell age, the survival data for uncorrelated deuteron ions were actually pooled from more than one experiment performed on different days. This was done because these data fitted to Eq. (7) separately did not yield values α_∞ and k significantly different from one another. The analysis has been based on the assumption of one common value k for the uncorrelated deuterons and the He ions. Figures 3 and 4 represent the data and their fit by the curves that correspond to the values given in Table I. Essentially the same fit is obtained for late S cells if a common value k is not postulated. For G_1/S cells an improved overall fit results in a larger value k for the ^{3}He ions and accordingly in a ratio α_0/α_∞ that is substantially smaller than 2 (see Appendix). However, this fit is poor for the low-dose points that determine α_0 for the ^{3}He ions. A direct fit to the low-dose points supports the value $\alpha_0/\alpha_\infty = 2$. Further support for the ratio $\alpha_0/\alpha_\infty = 2$ both for late S-phase and for G_1/S cells is given in recent track segment experiments with synchronized cells (*13*), where the initial slope of the survival curves increases by roughly a factor of 2 when the LET changes from 33 to 66 keV/μm. Earlier experiments on nonsynchronized cells[5] (*14*) had led to essentially the same result.

For finite separations b the ratios ξ_b/ξ_∞ are considerably less than 2. This means that little combination of sublesions occurs between the two tracks of correlated ions even if their mean separation is only 0.09 μm. For G_1/S cells the statistical

[5] P. W. Todd, *Reversible and Irreversible Effects of Ionizing Radiations on the Reproductive Integrity of Mammalian Cells Cultured in Vitro*. Thesis, University of California, Lawrence Rad. Lab., UCRL 11614 (1964).

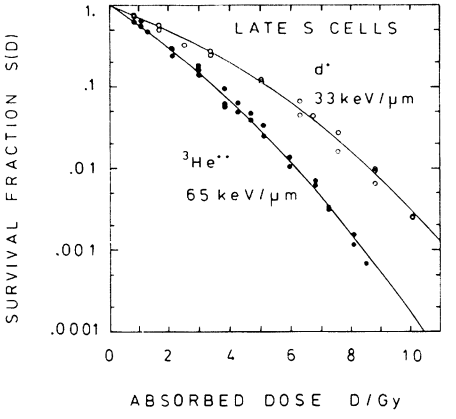

FIG. 3. Survival curves for late S-phase cells irradiated either with uncorrelated deuterons or ^{3}He ions of twice the LET, as indicated in the diagram. The solid curves through the data are fits corresponding to the parameters in Table I.

uncertainties are too large to permit the conclusion that the ratios are significantly larger than 1. For late S cells a one-sided t test shows that taken together the three values ξ_b for finite b exceed ξ_∞ with significance level 96%. That there is a real increase of the effect for the correlated particles agrees with the conclusions drawn from the more detailed presentation of the data (*3*).

From the simple site model and the value ξ of roughly 10 Gy for uncorrelated deuterons one would have inferred combination distances of the order of 1 μm, and one would have further concluded that combination of sublesions from two deuteron tracks would be very likely if these were separated by distances of the order of 0.1 μm. However, the data show that there is, in fact, relatively small interaction between the tracks of correlated ions and one must therefore ask

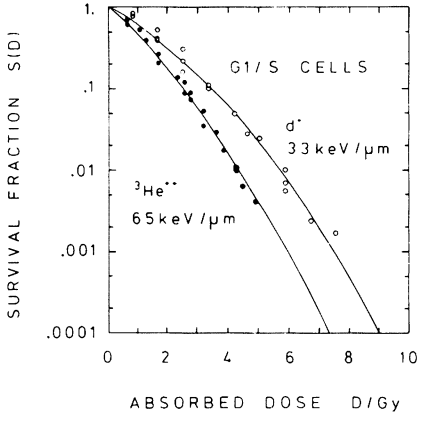

FIG 4. Survival curves for G_1/S-phase cells irradiated either with uncorrelated deuterons or ^{3}He ions of twice the LET, as indicated in the diagram. The solid curves through the data are fits corresponding to the parameters in Table I.

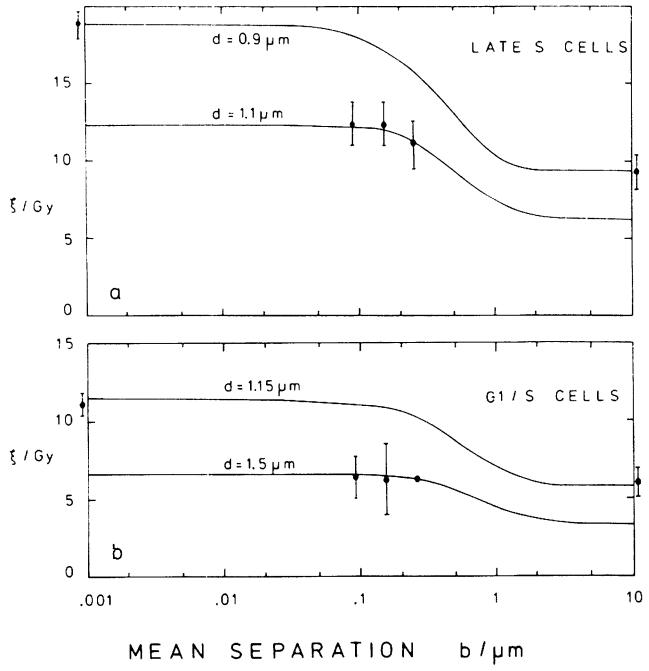

FIG. 5. The ratio ξ of the linear and the quadratic coefficient in the survival curves as a function of mean separation b of the correlated deuterons. The values for the uncorrelated deuterons are given on the right-hand border of the diagrams, the values for tracks are given on the left border of the diagram. The standard deviations correspond to the uncertainty of the coefficient α of the linear term. A joint value of k is used for all curves (see Table I). The curves represent the theoretical values ξ that result from the simple site model [Eqs. (8) and (10)]. With these equations no agreement with the data can be achieved.

whether this refutes the basic tenets of dual radiation action or whether a function $\gamma(x)$ exists that is consistent with the data.

INTERPRETATION OF THE RESULTS

In Figs. 5a and b the values ξ_b for the cells in late S phase and in G_1/S are given as solid dots together with standard deviations.

Figure 5 includes, on the right border, the value for uncorrelated deuterons. In addition the value is given for uncorrelated ^{3}He ions with LET = 65 keV/μm; this point is plotted at the left border of the diagram. The dose–effect relations for the deuterons and the ^{3}He ions are, as stated, fitted with the same k value of 0.030 Gy^{-2} for late S cells and 0.069 Gy^{-2} for G_1/S cells.

The site model in its conventional form (sublesions uniformly produced within a sphere of diameter d and interaction probability independent of separation) corresponds, as has been shown (*5*), to the following function $\gamma(x)$:

$$\gamma(x) = \left(1 - \frac{3x}{2d} + \frac{x^3}{2d^3}\right) \Big/ \frac{\pi\rho d^3}{6} \qquad \text{for} \qquad x \leq d. \tag{10}$$

Integrating Eq. (8) with this function $\gamma(x)$ as shown in Fig. 6 one obtains the curves in Fig. 5 for the specified site diameters. All the resulting curves show the expected increase of ξ by a factor of 2, as b decreases from large values to values that are small compared to d. It is readily apparent that the experimental data are not in agreement with the computed curves for any selected site diameter. According to the site model the observed values ξ_∞ correspond to a site diameter of 0.9 and 1.15 μm for late S and for G_1/S cells; this is also in agreement with the values ξ_0 for ^{3}He ions. However, the values ξ_b for the paired deuterons would in all cases have to be considerably larger than the values actually observed. The site model is therefore inconsistent with the data and other functions $\gamma(x)$ have to be examined.

In the present experiment only three different mean separations of the paired deuterons were applied, and it may be expected that there are various functions $\gamma(x)$ that may lead to equal agreement with the observed values ξ_b. In particular this appears likely if one admits the possibility that the probability of two transfers to produce a lesion had a complicated nonmonotonous dependence on distance. While such a possibility cannot in principle be excluded, there is little evidence to support it. For the present analysis it will therefore be assumed that $\gamma(x)$ is a smooth and monotonically decreasing function of distance. With this constraint one can ask for that function $\gamma(x)$ that fulfills the least-squares condition:

$$\sum \left[\int_0^\infty \gamma(x) t_b(x) dx - \xi_b \right]^2 \Big/ \sigma_b^2 = \text{minimum} \tag{11}$$

(summation over all five points in Fig. 5a or b).

By numerical optimization with the additional constraint that $\gamma(x)$ be a convex function (from above) in the logarithmic plot the function $\gamma(x)$ depicted in Figs. 7a and b as broken lines have been obtained for late S and G_1/S cells. The numerical procedure that has been utilized is the method of the generalized reduced gradient (*15*) in the computer version of Abadie (*16*). The resulting functions $\gamma(x)$ are de-

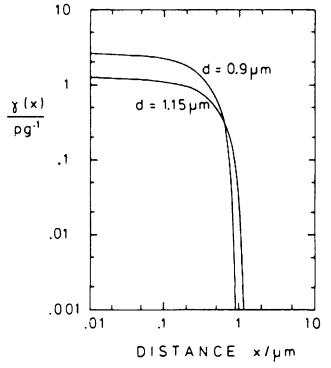

FIG. 6. The functions $\gamma(x)$ that correspond to the site model [see Eq. (10)]. The resulting curves for ξ are given in Fig. 5. The function $\gamma(x)$ has the dimension of reciprocal mass; the unit picogram (pg) is used because it leads to convenient numerical values and also because with density $\rho = 1$, it corresponds to 1 μm^3.

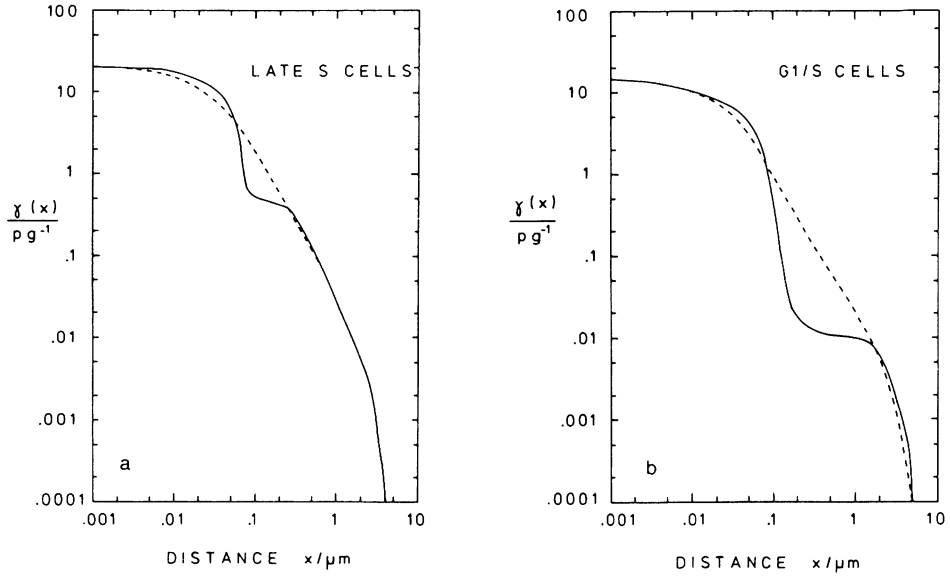

FIG. 7. The functions $\gamma(x)$ that lead to the best fit [see Eq. (11)] of the experimental data. The broken lines provide the best fit if one considers only curves that are convex (from above) in the logarithmic representation. A somewhat improved fit is obtained with the solid lines that do not meet this constraint. The fit obtained with these functions $\gamma(x)$ is represented in Fig. 8.

picted in Figs. 8a and b by the broken lines. These lines are consistent with the observed values ξ_b within the statistical errors of the observations.

It is apparent that no statements can be made on the actual form of the function $\gamma(x)$ at very small distances. The main result is therefore the strikingly wide range of interaction distances. According to the functions $\gamma(x)$ the probability of two energy transfers to form a lesion extends up to several micrometers; however, its value must be several orders of magnitude larger if the transfers occur at a separation of the order of 10 nm. This steep increase of the interaction function at small distances follows from the limited interaction between correlated tracks. However, it must be noted that the small but finite interaction probabilities at large distances are equally real. They follow from the presence of a substantial quadratic component in absorbed dose, i.e., from the low absolute values of ξ. Sufficient agreement with the experimental data can be achieved only with functions that reach up to a limit of at least 2 μm. If the upper limit is chosen to be 1 μm, no function $\gamma(x)$ exists that leads to even an approximate agreement with the experimental data. This means that no model based exclusively on short-range combination of sublesions is consistent with the observation of a substantial shoulder of the survival curve that is due to the interaction of independent particle tracks. This statement applies regardless of the geometry of the sensitive matrix in the cell and regardless of the form of the distance dependence for the combination of sublesions.

The precise form of $\gamma(x)$ may differ from that given by the broken lines in Figs. 7a and b. Thus one obtains a somewhat improved fit to the data and somewha: dif-

ferent functions $\gamma(x)$ if one abandons the constraint of convexity and requires merely that $\gamma(x)$ is a smooth monotonic function. With this relaxed constraint one obtains the solid curves in Figs. 7a and b for $\gamma(x)$ and the fit to the data that is indicated by the solid curves in Figs. 8a and b.

The statistical uncertainty of the data is too large to permit the statement that the solid lines in Fig. 7 are valid rather than the broken lines. Nevertheless it is of interest to note that these functions are similar to functions $\gamma(x)$ that would result if DNA were the target and if it were distributed randomly over an extended region of diameter d (several micrometers) in the nucleus of the cell in floccules that have smaller diameters δ (up to 100 nm). For spherical floccules randomly distributed in a spherical site of diameter d one would obtain the function

$$\gamma(x) \sim (1 - q)\left(1 - \frac{3x}{2\delta} + \frac{x^3}{2\delta^3}\right) + q \cdot \left(1 - \frac{3x}{2d} + \frac{x^3}{2d^3}\right). \tag{12}$$

q is the product of the fraction of the larger volume filled with floccules of sensitive material and a factor that accounts for a possible reduction of the combination probability of sublesions from different floccules compared to that in the same DNA floccule. The first term extends to $x = \delta$, the other term to $x = d$.

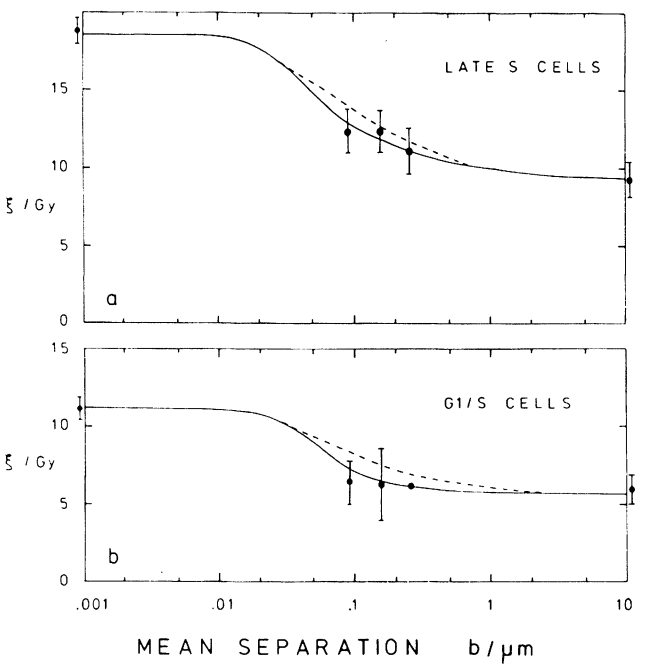

FIG. 8. The same representation of the experimental results as in Fig. 5. The solid curves represent the theoretical values that result from the functions $\gamma(x)$ that have been obtained by numerical optimization and that are represented by the solid curves in Fig. 7. The broken lines correspond to the broker curves in Fig. 7 that provide the best fit if one admits only functions $\gamma(x)$ that are convex (from above) in the logarithmic plot of Fig. 7.

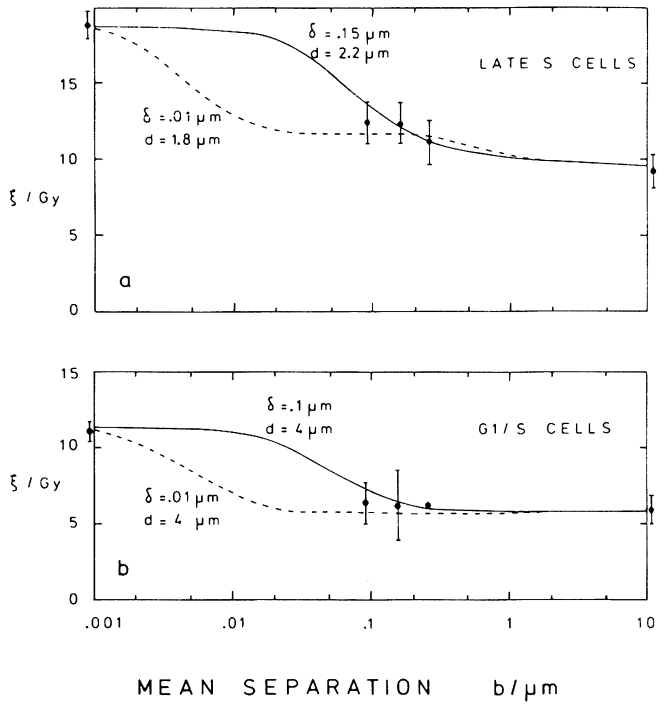

FIG. 9. The same representation of the experimental results as in Figs. 5 and 8. The curves are the theoretical values that result if small spherical targets of diameter δ are randomly distributed in a larger spherical site of diameter d [see Eq. (12)]. Both the solid and the broken curves are consistent with the data; the possibility of values δ much less than 0.1 μm can therefore not be rejected.

Figures 9a and b show fits that are obtained with functions $\gamma(x)$ corresponding to Eq. (15). Due to the statistical uncertainties of the data, different values of δ and d can lead to acceptable fits. All fits are somewhat inferior to that obtained with the functions $\gamma(x)$ from Fig. 7, and, in fact, no full agreement would be expected as the model is clearly a simplification. Nevertheless acceptable agreement is obtained if clusters of diameter $\delta = 0.15$ μm in a larger domain of diameter 2.2 μm are assumed for late S cells, and if clusters of diameter $\delta = 0.1$ μm in a larger domain of 4 μm diameter are assumed for G_1/S cells. However, it is also found that the possibility of much smaller clusters (diameter $\delta \sim 0.01$ μm) in the larger domains cannot be rejected, especially in the case of G_1/S cells where the interaction of correlated tracks is not established with statistical significance. Further data would be necessary to decide this point; it would also be necessary to account for δ-ray structure, if a rigorous analysis at small values x were attempted.

One must therefore conclude that the precise form of the functions $\gamma(x)$ cannot be given with certainty. However, the essential finding is valid, the interaction function $\gamma(x)$ declines sharply at small separations, there is interaction between correlated tracks at least for late S cells, and there must be long-range interactions between independent tracks.

CONCLUSIONS

The data presently available from the experiment are limited and are subject to considerable statistical uncertainties. Nevertheless, two definite conclusions are possible. First, the ratio of the linear to the quadratic component in the survival curves of late S-phase cells is of the order of 10 Gy for the uncorrelated deuterons and of the order of 20 Gy for the helium ions that have twice the stopping power and can therefore be assumed to be roughly equivalent to two coinciding deuteron tracks. For G_1/S cells the values are smaller (5.5 and 11 Gy). Second, with correlated deuterons only a small increase of the effect occurs even if the mean lateral separation of these correlated deuterons is as small as 0.1 μm. Various functions $\gamma(x)$ can be considered that represent the effectiveness of a pair of energy transfers to create sublesions which then in turn interact to form a lesion. However, no function $\gamma(x)$ leads to values ξ as low as 10 or 20 Gy for the deuterons or the helium ions if it does not extend to distances x of roughly 1 μm. On the other hand, it is found that even a separation of 0.1 μm of two correlated tracks leads to a substantial loss of intertrack interactions; two tracks separated by 0.1 μm are considerably less effective than the helium ion that represents two coinciding tracks. This implies that the function $\gamma(x)$ must decline sharply at distances less than 0.1 μm. The actual numerical analysis has resulted in estimated curves $\gamma(x)$ that show this property of declining sharply with distance x while reaching out, with small probability, to large combination distances.

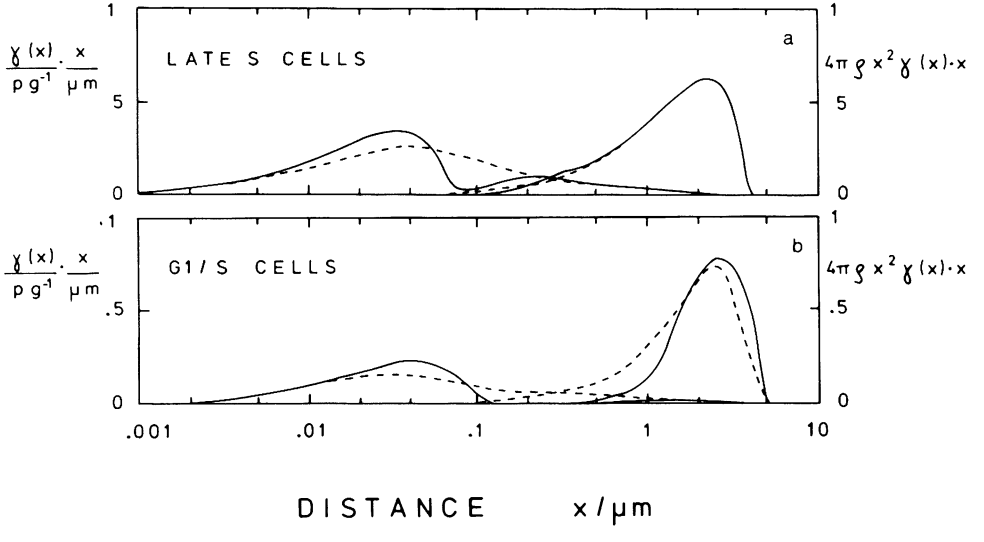

FIG. 10. Distributions of initial separations of combining sublesions for the cells in late S phase and in G_1/S. In each case distributions are given separately for the linear (intratrack) and the quadratic (intertrack) terms. The distributions are per unit log-interval so that equal areas correspond to equal frequencies. The ordinate is given in arbitrary units, but the relative contribution of the intratrack and the intertrack mechanism is correctly represented for single deuterons (L = 32 keV/μm) at an absorbed dose L of 10 Gy. The intratrack term is proportional to LD, the intertrack term to D^2. The solid and the broken curves correspond to the solid and the broken curves in Fig. 7.

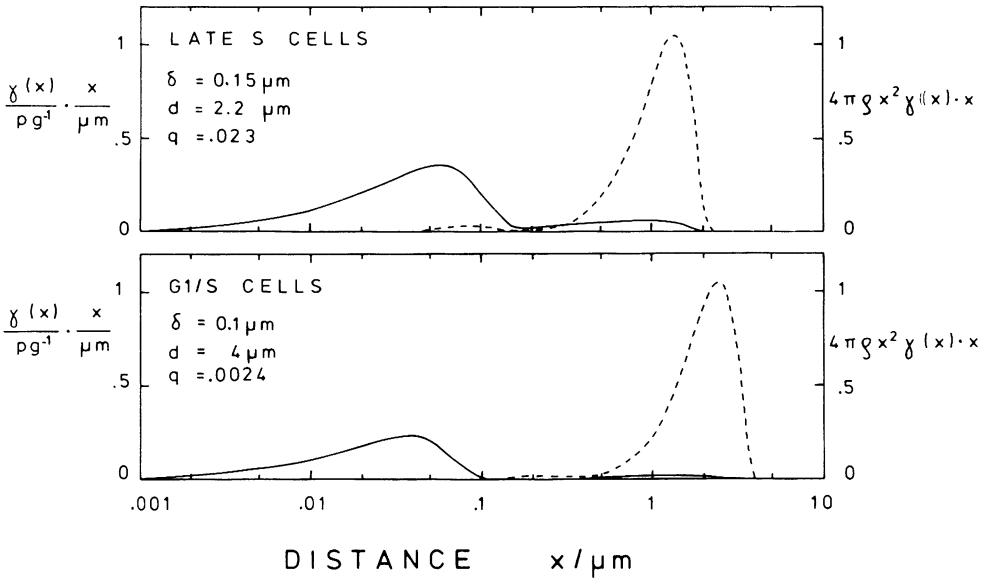

FIG. 11. Distributions of initial separations of combining sublesions that correspond to a random distribution of spherical targets of diameter δ in a larger region d. The distributions for the intratrack component are, in this diagram, given by solid lines, the distributions for the intertrack mechanism by broken lines. The curves correspond to the same functions $\gamma(x)$ that lead to the solid lines in Fig. 9. The representation is analogous to that in Fig. 10.

For a linear track of stopping power L one has at a distance x to $x + dx$ from an energy transfer an expected energy transfer from the same track equal to $2\ Ldx$. The expected energy transfer from unrelated tracks is $4\pi\rho x^2 Ddx$. Using these values and the function $\gamma(x)$ one concludes that the frequency of *intra*track combinations at different separations x is proportional to $\gamma(x) \cdot LD$, while the frequency of *inter*track combinations is proportional to $4\pi\rho x^2 \gamma(x) D^2$. The functions in Fig. 7 then lead to the frequency distributions in initial separation of interacting transfers that are represented in Figs. 10a and b for late S-phase cells and for G_1/S cells. These functions contain the additional factor x that accounts for the logarithmic scale and preserves the areas under the curves. The intratrack term is proportional to the area under the left-hand peaks; the intertrack term is proportional to the area under the right-hand peaks. The relative contribution of the linear intratrack term and the quadratic intertrack term is correctly represented for single deuterons (L = 32 keV/μm) at an absorbed dose D of 10 Gy.

The striking conclusion from Fig. 10 is the large difference in combination distances for the intratrack and the intertrack effect. Combination of sublesions *within* particle tracks appears to take place predominantly at distances below 0.1 μm, while the combination of sublesions from different particle tracks must be almost exclusively due to interactions in the micrometer range.

The possibility has been considered that the sensitive matrix in the cell consists of floccules of DNA distributed over a larger region in the cell nucleus. If this is so, one would have to conclude that the linear intratrack term involves mainly

single floccules, while the quadratic intertrack term involves mostly two DNA floccules. Figure 11 can illustrate this. This figure is analogous to Fig. 10. However, it corresponds to the solid lines in the fit that is represented in Fig. 9 and that results from the assumption of small spherical targets distributed over larger domains. This figure is given in addition to Fig. 10 to emphasize again the point that the exact dependence of the combination probability of sublesions on distance cannot be deduced from the present experiment, while the substantial difference of interaction distances for the intratrack and the intertrack mechanism is well established.

It is of interest to note that in recent experiments with the radioprotector DMSO Chapman *et al.* (*17*) have shown characteristic differences in the dose-modifying factors that apply to the linear and the quadratic component in the survival curve. The linear component appears to be more strongly affected than the quadratic component. This could be linked to the fact that the intratract effect is initiated simultaneously by the same particle track, while the sublesions involved in the quadratic effect are produced with a certain temporal separation. However, the authors have considered the additional possibility that their results reflect smaller interaction distances for the linear, one-particle effect and larger interaction distances for the quadratic, two-particle effect. This assumption is in line with the conclusions of the present analysis.

Although the "distance model" was considered in the original publication (*4*), the simpler "site model" has frequently been employed. The results of the molecular ion experiment show that the concept of dual radiation action, i.e., the pair-wise interaction of sublesions, cannot be applied to cell survival in the form of the site model, but they are consistent with the generalized formulation of the distance model (*5*).

An alternate explanation of the kinetics of cellular radiation effects in general is based on the concept of dose-dependent repair. This concept has been invoked to account for the presence of the shoulder of the survival curve. If the initial damage required highly localized energy transfer it certainly would be expected that even slight separations between tracks result in substantial increase of survival. It might also be argued that the capacity for repair of the damage produced by a single track is somewhat impaired by the presence of another track that is separated by distances of the order of 100 nm or even more; this could explain the degree of synergism that has been found for the correlated ions, and a general dose-dependent decrease of repair capacity could finally account for the observed nonlinear component in the dose–effect relations. However, there is at present no formulation of the concepts that permits a quantitative explanation. Furthermore, the repair model does not account for the second order kinetics of cellular inactivation and of various other cellular effects which is clearly indicated by the dependence of RBE on radiation quality and on absorbed dose (*4*).

APPENDIX: DETERMINATION OF THE SURVIVAL CURVE PARAMETERS

In the present experiments it has not been possible to obtain full survival curves simultaneously. Even for the uncorrelated deuterons and the ^{3}He ions it has been necessary to utilize data obtained in successive experiments. This, together with

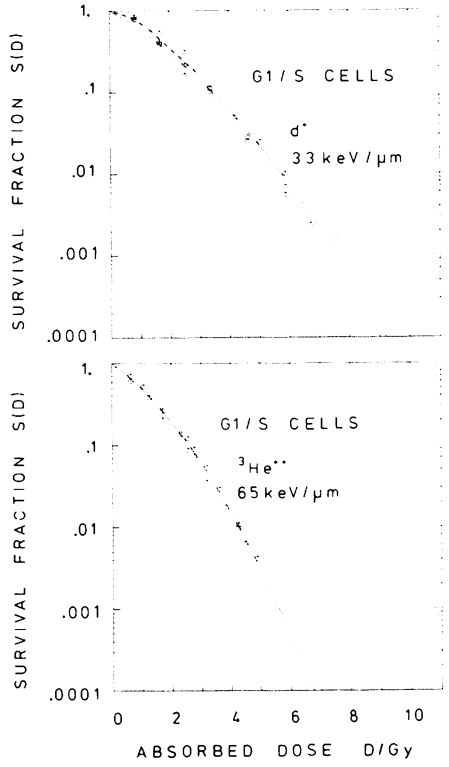

FIG. 12. The same survival data as in Fig. 4 fitted to linear-quadratic relations with different coefficients β. The least-squares fit is obtained with $\alpha = 0.47\ Gy^{-1}$ and $\beta = 0.057\ Gy^{-2}$ for the deuterons, and $\alpha = 0.61\ Gy^{-1}$ and $\beta = 0.11\ Gy^{-2}$ for the ^3He ions. The broken curve segment in the plot for deuterons indicates the inadequacy of the least-squares fit in this dose range.

some of the constraints of the irradiation setup, leads to fluctuations in the survival curves that exceed those attainable under optimal conditions. The statistical analysis of the survival curves in Figs. 3 and 4 may therefore be of limited validity. This is particularly true for the G_1/S data that show considerable fluctuations.

For these reasons, it is uncertain whether individual fits to the survival curves can lead to reliable conclusions on a possible dependence of the coefficient k on LET. It may nevertheless be helpful to consider the numerical results that are obtained by such individual fits.

For late S cells it is found that the individual fits lead to values k (0.028 and 0.034 Gy^{-2}) similar to the joint value of 0.03 Gy^{-2}. The values of α (0.26 and 0.54 Gy^{-1}) are also close to the values obtained in the joint fit (0.28 and 0.56 Gy^{-1}). All values are consistent with the values quoted in the earlier article (*3*) that was based on nearly the same set of data points.

For G_1/S cells the results are less consistent. A separate fit (see Fig. 12) leads to values k (0.057 and 0.11 Gy^{-2}) that differ widely from the value $k = 0.069\ Gy^{-2}$ from the joint fit. The values of α (0.47 and 0.61 Gy^{-1}) deviate correspondingly from the values (0.41 and 0.76 Gy^{-1}) of the joint fit.

A comparison of the curves in Figs. 3 and 4 with those in Fig. 12 and a consideration of the large fluctuations in the data points make it very uncertain whether the results of the separate fits are reliable. In particular, there is in Fig. 12 substantial disagreement of the fit with the low-dose points for the 33 keV/μm deuterons. As shown by the broken curve segment, the low-dose points indicate a much smaller value of the initial slope. For this reason a joint k, even for G_1/S cells, has not been rejected in the analysis, and the data in Table I have been used. It must, however, be noted that this introduces an element of uncertainty into the analysis that would require improved experimental data for G_1/S cells.

ACKNOWLEDGMENTS

This investigation was supported by Contract DE-AS02-78EV04733 from the Department of Energy and by Grant CA 12536 to the Radiological Research Laboratory/Department of Radiology, and by Grant CA 13696 to the Cancer Center/Institute of Cancer Research, awarded by the National Cancer Institute, DHEW.

RECEIVED: August 24, 1979; REVISED: April 17, 1980

REFERENCES

1. H. H. ROSSI, Biophysical studies with spatially correlated ions. 1. Background and theoretical considerations. *Radiat. Res.* **78,** 185–191 (1979).
2. R. D. COLVETT and N. ROHRIG, Biophysical studies with spatially correlated ions. 2. Multiple scattering, experimental facility, and dosimetry. *Radiat. Res.* **78,** 192–209 (1979).
3. R. P. BIRD, Biophysical studies with spatially correlated ions. 3. Cell survival studies using diatomic deuterium. *Radiat. Res.* **78,** 210–223 (1979).
4. A. M. KELLERER and H. H. ROSSI, The theory of dual radiation action. *Curr. Top. Radiat. Res. Q.* **8,** 85–158 (1972).
5. A. M. KELLERER and H. H. ROSSI, A generalized formulation of dual radiation action. *Radiat. Res.* **75,** 471–488 (1978).
6. D. CHMELEVSKY, A. M. KELLERER, and H. H. ROSSI, Concepts and quantities relevant to the evaluation of charged particle tracks. In *Sixth Symposium on Microdosimetry* (J. Booz and H. G. Ebert, Eds.), Vol. II, pp. 855–868. Commission of the European Communities, Harwood, London, 1978. [EUR 6064 d-e-f.]
7. G. ALM CARLSSON, Basic concepts in dosimetry. A critical analysis of the concepts of ionizing radiation and energy imparted. *Radiat. Res.* **75,** 462–470 (1978).
8. C. R. GEARD, R. D. COLVETT, and N. ROHRIG, On the mechanics of chromosomal aberrations: A study with single and multiple spatially-associated protons. *Mutat. Res.* **69,** 81–99 (1980).
9. W. GROSS and A. M. KELLERER, The mean spacing of protons arising from molecular ions. In: *Annual Report on Research Project*, Radiation Research Laboratory, Columbia University, pp. 152–159, 1973. [Available as USAEC COO-3243-2 from National Technical Information Service, Springfield, VA 22161.]
10. D. CHMELEVSKY, *Distributions et moyennes des grandeurs microdosimétriques à l'échelle du nanomètre.* Report CEA-R-4785, 1976. [Available from the Commissariat a L'Energie Atomique, France.]
11. A. M. KELLERER, E. J. HALL, H. H. ROSSI, and P. TEEDLA, RBE as a function of neutron energy. II. Statistical analysis. *Radiat. Res.* **65,** 172–186 (1976).
12. A. M. KELLERER and J. BRENOT, On the statistical evaluation of dose-response function. *Radiat. Environ. Biophys.* **11,** 1–13 (1974).
13. R. P. BIRD, N. ROHRIG, R. D. COLVETT, C. R. GEARD, and S. A. MARINO, Inactivation of synchronized Chinese hamster V79 cells with charged-particle track segments. *Radiat. Res.* **82,** 277–289 (1980).

14. G. W. BARENDSEN, Mechanism of action of different ionizing radiations on the proliferative capacity of mammalian cells. In *Theoretical and Experimental Biophysics* (A. Cole, Ed.), Vol. 1, pp. 167–231. Dekker, New York, 1967.

15. D. M. HIMMELBLAU, *Applied Nonlinear Programming*. McGraw–Hill, New York, 1972.

16. J. ABADIE, Numerical experiments with the GRG method. In *Integer and Non-linear Programming*. North-Holland, Amsterdam, 1970.

17. J. D. CHAPMAN, S. D. DOERN, A. P. REUVERS, C. J. GILLESPIE, A. CHATTERJEE, E. A. BLAKELY, K. C. SMITH, and C. A. TOBIAS, Radioprotection by DMSO of mammalian cells exposed to X-rays and to heavy charged-particle beams. *Radiat. Environ. Biophys.* **16**, 29–41 (1979).

18. M. J. BERGER, Beta-ray dosimetry calculations with the use of point kernels. In *Medical Radionuclides: Radiation Dose and Effects* (R. J. Cloutier, C. L. Edwards, and W. S. Snyder, Eds.), pp. 63–86, 1970. [Available as USAEC Report CONF-691212 from National Technical Information Service, Springfield, VA 22161.]